Pilot Designs and Compensation Scheme for Severe RF Distortions in Millimeter-Wave Massive MIMO Systems

A. Khansefid[1], H. Minn[1], N. Al-Dhahir[1], H. Huang[2], and X. Du[2]
[1] The University of Texas at Dallas, Richardson, TX, USA
[2] Huawei Technologies Co., Ltd., Shenzhen, China

***Abstract*—Emerging millimeter-wave massive MIMO systems are subject to strong radio frequency (RF) distortions and their compensation is crucial to meet the high performance targets of such systems. This paper presents novel pilot designs and related estimators for multi-input multi-output (MIMO) millimeter-wave systems characterized by frequency-selective channels, mirror interference, and time-varying inter-carrier interferences at both the transmitter and receiver. The bit error rate (BER) simulation results illustrate that our proposed designs achieve substantially lower BER than reference pilot designs in the literature.**

***Index Terms*—millimeter-wave, RF imperfection, phase noise, IQ imbalance, carrier frequency offset**

I. Introduction

Millimeter-wave systems are gaining increased interest [1] but suffer from strong RF distortions. Pilot signals are commonly used for channel estimation and RF distortion compensation. There exist several pilot designs for channels with RF distortions in the literature, mainly in three groups: 1) pilot designs for channels with in-phase and quadrature-phase imbalance (IQI) [2]–[8], 2) those for channels with phase noise (PN) or PN plus carrier frequency offset (CFO) [9], and 3) those for channels with IQI and PN [10], [11].

The above pilot designs consider either some of the RF distortions or small RF distortion levels, or RF distortions at either transmitter (TX) or receiver (RX) side. Existing pilot designs for systems with IQI exploit mirror tone interference (MTI). However, when the PN level is high, inter-carrier interference (ICI) arises which affects MTI and degrades the performance of those pilot designs. Existing pilot designs for PN-impaired systems focus on capturing the PN-induced common phase error (CPE) or its combined effect with the channel. But under IQI, MTI causes substantially degraded performance to the pilot designs. Existing pilot designs for systems with IQI and PN assume small PN level at the receiver side only such that no significant ICI occurs. Some of the existing works rely on the unjustified assumption of perfect knowledge of the channels without taking RF distortions into account. In summary, for systems with high levels of RF distortions such as IQI and strong PN at both TX and RX sides, all existing pilot designs are not suitable and new pilot designs capable of handling such high RF distortions are needed.

In this paper, we consider an orthogonal frequency division multiplexing (OFDM) system with strong PN, fractional CFO, and IQI at both the TX and RX sides. We propose a set of pilot designs and estimators for this system. Simulation results show advantages of the proposed designs.

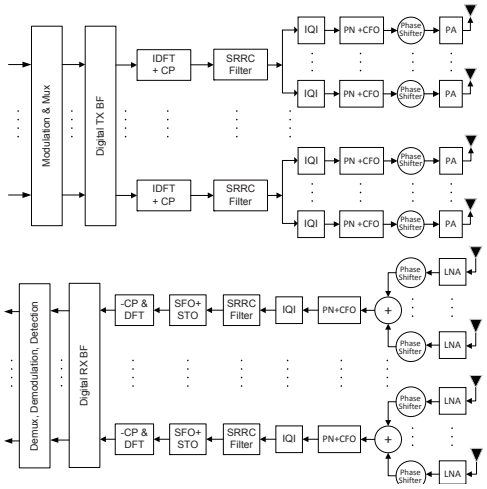

Fig. 1. Downlink MIMO-OFDM signal model block diagram with RF impairments. (SRRC = square-root raised cosine filter, PA = power amplifier, LNA = low-noise amplifier, SFO = sampling frequency offset, STO = sampling time offset, BF = beam-forming, CP = cyclic prefix)

Notation: Vectors (matrices) are denoted by bold face lower (upper) case letters. The superscripts * and T stand for conjugate and transpose. $\Re\{\cdot\}$ and $\Im\{\cdot\}$ denote real part and imaginary part. $\lceil\cdot\rceil$ is the ceiling operation.

II. Signal Model

We consider an OFDM downlink (DL) system. The base station (BS) has U_T digital-to-analog conversion (DAC) branches and each branch is connected to V_T antenna elements (i.e., hybrid beamforming architecture for complexity saving). Similarly, user equipment (UE) has U_R analog-to-digital conversion (ADC) branches and each branch is connected to V_R antenna elements. Fig. 1 shows the system block diagram.

Suppose there are N used subcarriers with indexes $k_1, \cdots, k_N$ where $k_i = -k_{N-i}$ and k_i for $i \leq N/2$ are negative. Define the frequency-domain signal vector at the TX DAC branch u_1 as $\mathbf{C}_{u_1} \triangleq [C_{u_1}[k_1], \cdots, C_{u_1}[k_N]]^T$ and that at the receive ADC branch u_2 as $\mathbf{Y}_{u_2} \triangleq [Y_{u_2}[k_1], \cdots, Y_{u_2}[k_N]]^T$. We can model the frequency-domain signal for one OFDM symbol with N used sub-carriers as

$$\mathbf{Y}_{u_2} = \sum_{u_1=1}^{U_T} \mathbf{A}_{u_2u_1}\mathbf{C}_{u_1} + \mathbf{B}_{u_2u_1}\mathbf{C}^*_{u_1} + \mathbf{W}_{u_2} \qquad (1)$$

where $\mathbf{A}_{u_2u_1}$ and $\mathbf{B}_{u_2u_1}$ are components of the equivalent channel in the presence of RF distortions, and $\mathbf{W}_{u_2}$ is the

978-1-5090-2482-7/16/$31.00 ©2016 IEEE

noise vector. The significant elements of $\mathbf{A}_{u_2u_1}$ (due to channel, PN and CFO effects) would be around the main diagonal, thus taking a banded diagonal form while those of $\mathbf{B}_{u_2u_1}$ (due to IQI) would be around the anti-diagonal.

Define $\mathbf{C}_{R,u_1} \triangleq \Re\{\mathbf{C}_{u_1}\}$, $\mathbf{C}_{I,u_1} \triangleq \Im\{\mathbf{C}_{u_1}\}$, $\mathbf{Y}_{R,u_2} \triangleq \Re\{\mathbf{Y}_{u_2}\}$, $\mathbf{Y}_{I,u_2} \triangleq \Im\{\mathbf{Y}_{u_2}\}$, $\tilde{\mathbf{Y}}_{u_2} \triangleq [\mathbf{Y}_{R,u_2}^T, \mathbf{Y}_{I,u_2}^T]^T$, $\tilde{\mathbf{C}}_{u_1} \triangleq \left[\mathbf{C}_{R,u_1}^T, \mathbf{C}_{I,u_1}^T\right]^T$, $\boldsymbol{\eta}_{u_2} \triangleq \left[\Re\{\mathbf{W}_{u_2}\}^T, \Im\{\mathbf{W}_{u_2}\}^T\right]^T$, and

$$\mathbf{U}_{u_2u_1} \triangleq \mathbf{A}_{u_2u_1} + \mathbf{B}_{u_2u_1} \tag{2}$$

$$\mathbf{V}_{u_2u_1} \triangleq j(\mathbf{A}_{u_2u_1} - \mathbf{B}_{u_2u_1}). \tag{3}$$

Then we can express (1) in the real-valued form as

$$\tilde{\mathbf{Y}}_{u_2} = \sum_{u_1=1}^{U_T} \mathbf{Q}_{u_2u_1}\tilde{\mathbf{C}}_{u_1} + \boldsymbol{\eta}_{u_2} \tag{4}$$

where $\mathbf{Q}_{u_2u_1}$ is given by

$$\mathbf{Q}_{u_2u_1} \triangleq \begin{bmatrix} \Re\{\mathbf{U}_{u_2u_1}\} & \Re\{\mathbf{V}_{u_2u_1}\} \\ \Im\{\mathbf{U}_{u_2u_1}\} & \Im\{\mathbf{V}_{u_2u_1}\} \end{bmatrix}. \tag{5}$$

In (4), the effective channel between DAC branch u_1 and ADC branch u_2 is given by $\mathbf{Q}_{u_2u_1}$ which is a $2N \times 2N$ matrix. Finally, collecting the frequency-domain signal vectors from all ADC branches, the signal model can be expressed as

$$\tilde{\mathbf{Y}} = \mathbf{Q}\tilde{\mathbf{C}} + \boldsymbol{\eta} \tag{6}$$

where $\tilde{\mathbf{Y}} \triangleq \left[\tilde{\mathbf{Y}}_1^T \cdots \tilde{\mathbf{Y}}_{U_R}^T\right]^T$, $\tilde{\mathbf{C}} \triangleq \left[\tilde{\mathbf{C}}_1^T \cdots \tilde{\mathbf{C}}_{U_T}^T\right]^T$, $\boldsymbol{\eta} \triangleq \left[\boldsymbol{\eta}_1^T \cdots \boldsymbol{\eta}_{U_T}^T\right]^T$ and the (m,k) sub-matrix of $\mathbf{Q}$ is $\mathbf{Q}_{mk}$. $\mathbf{Q}$ is the equivalent channel matrix accounting for the channel, RF distortions, and analog beamforming. Later, we insert OFDM symbol index n to the signal model as $\mathbf{Y}_n$, $\mathbf{Q}_n$, $\mathbf{Q}_{ij,n}$, $\mathbf{A}_{u_2u_1,n}$, and $\mathbf{B}_{u_2u_1,n}$. Note that our signal model is also applicable to multi-user MIMO as we use different RF distortions for different ADC branches.

III. Pilot Design

Our pilot designs are different from the existing ones in terms of the locations of non-zero pilot tones and null tones. We allocate non-zero pilot tones and null tones such that any considered parameter estimation based on a relevant subset of tones is not (significantly) affected by any other non-zero pilots and data tones under the considered RF distortions.

First, we define the system parameters used in the pilot designs. OFDM uses a DFT size of N_{DFT} with the subcarrier spacing Δf, and the used subcarrier index range of $[-N_{\mathrm{L}}, N_{\mathrm{R}}]$. One-side spreads of significant ICI and MTI are κ subcarriers and ι subcarriers. The DC tone is not used and the first used subcarrier index to the right of the DC tone is denoted by l_1. Subcarrier index sets of non-zero pilot tones at the left and right side of the DC tone at OFDM symbol n are denoted by $J_{\mathrm{NZP},n}^{\mathrm{L}}$ and $J_{\mathrm{NZP},n}^{\mathrm{R}}$ with $J_{\mathrm{NZP},n} = \{J_{\mathrm{NZP},n}^{\mathrm{L}}, J_{\mathrm{NZP},n}^{\mathrm{R}}\}$. The mirror index set of $J_{\mathrm{NZP},n}$ is $J_{\mathrm{NZPM},n} = -J_{\mathrm{NZP},n}$. For digital channel k (kth spatial channel in a spatial multiplexing mode), the superscript (k) is added to the index sets. Index set of the combined non-zero and null pilots at the left sides of the DC tone at OFDM symbol n is denoted by $J_{\mathrm{P},n}^{L}$ and at the right side is $J_{\mathrm{P},n}^{\mathrm{R}}$. The effective channel coherence bandwidth is W_{coh} and its normalized version is $\rho \triangleq \left\lceil \frac{W_{\mathrm{coh}}}{\Delta f} \right\rceil$.

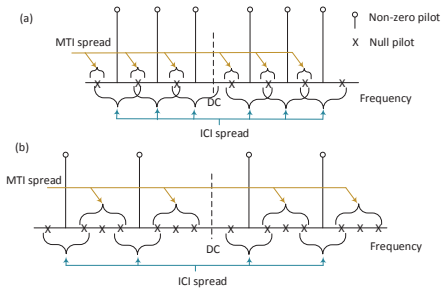

Fig. 2. The basic design approach for estimating main diagonal elements of $\mathbf{Q}_{ij}$. (a) $\kappa = 1$ and $\iota = 0$, (b) $\kappa = 1$ and $\iota = 1$

Next, we illustrate the basic concept of our pilot designs in Fig. 2 and Fig. 3 for different scenarios where the DC tone is not used and is denoted by the dashed line in the figures. In Fig. 2, the parameters of interest are the effective channel gains (the main diagonal elements of $\mathbf{Q}_{ij}$) and hence adjacent non-zero pilot tones at each side of the DC tone are spaced by $\max(\kappa+1, 2\iota+2)$ tones so that non-zero pilots are not affected by ICI spread and MTI spread of other non-zero pilots. In other words, $\max(\kappa, 2\iota+1)$ null pilot tones are inserted between adjacent non-zero pilot tones at each side of the DC tone and then the non-zero pilots at the positive subcarrier indexes and those at the negative indexes are positioned such that their respective MTI spreads fall on null pilot positions. The above spacing of $\max(\kappa+1, 2\iota+2)$ tones which avoids significant interference among non-zero pilots in estimating main diagonal elements of $\mathbf{Q}_{ij}$ will be called the minimum interference-free distance of non-zero pilot tones for the main diagonal elements; or in short form, $\mathrm{IFD}_{\mathrm{main}}$.

If the spacing of adjacent non-zero TX pilot tones is not larger than W_{coh}, one preamble symbol is sufficient to compute channel estimates of the used band. Otherwise, the above design approach is applied over several preamble symbols with appropriate shifting of the non-zero TX pilot tone indexes in each symbol so that collectively all the non-zero TX pilot tones of the preamble symbols cover the used band with adjacent tone spacing not larger than W_{coh}.

In Fig. 3, the parameters of interest are either both ICI and MTI coefficients or all parameters of the effective channel gains, ICI and MTI. We can observe in Fig. 3 that the ICI and MTI spreads of each non-zero pilot are decoupled and they are also not affected by ICI and MTI spreads of other non-zero pilot tones. In other words, $(2\kappa+2\iota+1)$ null pilot tones are inserted between adjacent non-zero pilots at each side of the DC tone and the pilots of both sides are positioned such that the locations of MTI spreads disjointly fall between the locations of ICI spreads. The non-zero pilot tones at each side have a spacing of $(2\kappa+2\iota+2)$ tones which will be called the minimum interference-free distance of non-zero pilot tones for the ICI and MTI elements; or in short form, $\mathrm{IFD}_{\mathrm{ICI,MTI}}$.

Next, we describe general design guidelines.

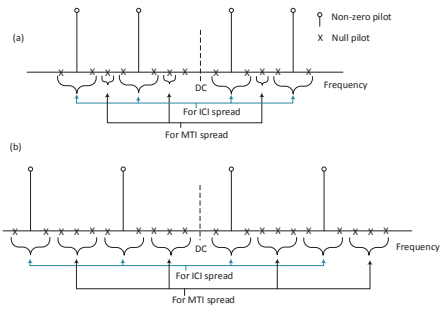

Fig. 3. The basic design approach for estimating effective channel gains, ICI and MTI coefficients. (a) $\kappa = 1$ and $\iota = 0$, (b) $\kappa = 1$ and $\iota = 1$

1) In all our designs, the non-zero pilot tones carry constant-amplitude sequences with low peak-to-average power ratio property, thus only their subcarrier indices need to be defined.

2) Depending on the criteria used, the values of κ, ι, and ρ can vary. Thus, to achieve the best BER, we propose to consider a few candidates $\kappa = \kappa_0 \pm m$, $\iota = \iota_0 \pm m$, and $\rho = \rho_0 \pm m$ where m is a non-negative integer starting from 0, and κ_0, ι_0, and ρ_0 are their initial values (described later). We can stop increasing m at a considered side ($+m$ side or $-m$ side) when BER increases at that side, and the final design is the one with the smallest BER. This approach will be applied to all the following pilot designs.

3) For scenarios with a boundary condition of two pilot designs, both designs should be tested.

4) The overhead ratio (with reference to the frame length) should also be considered. For example, it is not desirable to use more preamble symbols if it gives a slightly better BER but a notably larger overhead ratio.

Applying the basic approach mentioned before, we present next several pilot designs. In describing the subcarrier indexes, we will use the MATLAB's convention.

Design 1A: This is a preamble-type design for estimating the main diagonal elements of $\mathbf{Q}_{ij,n}$ for a single digital channel when $\rho > \mathrm{IFD}_{\mathrm{main}}$. Depending on the objective, e.g., for tracking time-varying channels, more than one OFDM symbol of preamble type can be interspersed within the transmission frame. Let n denote the symbol index of those pilot OFDM symbols. Then the pilot design is given by the non-zero pilot index sets at the left and right side of the DC tone as $J^L_{\mathrm{NZP},n} = -(l_1 + \iota + 1) : -D : -N_L$, $J^R_{\mathrm{NZP},n} = l_1 : D : N_R$ or $J^L_{\mathrm{NZP},n} = -l_1 : -D : -N_L$, $J^R_{\mathrm{NZP},n} = (l_1 + \iota + 1) : D : N_R$ where $D = \mathrm{IFD}_{\mathrm{main}} = \max(\kappa + 1, 2\iota + 2)$ and $J_{\mathrm{NZPM},n} \cap J_{\mathrm{NZP},n} = \emptyset$. In general, when $\rho > \mathrm{IFD}_{\mathrm{main}} + L$ for a non-negative integer L, we can set $D = \mathrm{IFD}_{\mathrm{main}} + k$ for any integer k with $0 \le k \le L$ subject to its performance.

Design 1B: This is a preamble-type design for estimating the main diagonal elements of $\mathbf{Q}_{ij,n}$ for K digital channels when $\rho > K \cdot \mathrm{IFD}_{\mathrm{main}}$. In the same way as in Design 1A, let n denote the symbol index of those pilot OFDM symbols. Then the pilot design is given by $J^{L,(1)}_{\mathrm{NZP},n} = -(l_1 + \iota + 1 + (K-1)D) : -D' : -N_L$, $J^{R,(1)}_{\mathrm{NZP},n} = l_1 : D' : N_R$, and $J^{(l)}_{\mathrm{NZP},n} = J^{(1)}_{\mathrm{NZP},n} + (l-1)D$ for $l = 2, 3, \cdots, K$ or $J^{L,(1)}_{\mathrm{NZP},n} = -l_1 : -D' : -N_L$, $J^{R,(1)}_{\mathrm{NZP},n} = (l_1 + \iota + 1 + (K-1)D) : D' : N_R$, $J^{(l)}_{\mathrm{NZP},n} = J^{(1)}_{\mathrm{NZP},n} - (l-1)D$ for $l = 2, 3, \cdots, K$, where $D = \mathrm{IFD}_{\mathrm{main}} = \max(\kappa + 1, 2\iota + 2)$, $D' = KD$, and $J_{\mathrm{NZPM},n} \cap J_{\mathrm{NZP},n} = \emptyset$ with $J_{\mathrm{NZP},n} = \cup_{l=1}^{K} J^{(l)}_{\mathrm{NZP},n}$ and $J_{\mathrm{NZPM},n} = \cup_{l=1}^{K} J^{(l)}_{\mathrm{NZPM},n}$. In general, when $\rho > K \cdot (\mathrm{IFD}_{\mathrm{main}} + L)$ for a non-negative integer L, we can set $D = \mathrm{IFD}_{\mathrm{main}} + k$ for any integer k with $0 \le k \le L$ subject to its performance.

Design 1C: This is a preamble-type design for estimating the main diagonal elements of $\mathbf{Q}_{ij,n}$ for K digital channels when $\mathrm{IFD}_{\mathrm{main}} < \rho < K \cdot \mathrm{IFD}_{\mathrm{main}}$. Define $K_0 = \lceil \rho / \mathrm{IFD}_{\mathrm{main}} \rceil$ and positive integers K_i such that $K_i \le K_{i-1}$ with $K_1 + K_2 + \cdots + K_M = K$. This design uses M OFDM preamble symbols where preamble symbol n carries pilots of K_n digital channels. At preamble symbol n, Design 1B with $K = K_n$ is applied. For example, if $K_0 = 2$ and $K = 5$, then we can set $K_1 = 2, K_2 = 2, K_3 = 1$, and $M = 3$. Any ordering of the values of K_i can be used as well.

Design 1D: This is a preamble-type design for estimating the main diagonal elements of $\mathbf{Q}_{ij,n}$ for a single digital channel when $\rho < \mathrm{IFD}_{\mathrm{main}}$. This design uses $M = \lceil \mathrm{IFD}_{\mathrm{main}} / \rho \rceil$ preamble symbols. In the first preamble symbol ($n = 1$), Design 1A is applied. Based on the pilot index sets at $n = 1$, the pilots at preamble symbol n, for $n = 2, \cdots, M$, are defined by $J_{\mathrm{NZP},n} = \beta_n + (n-1)\lfloor D/M \rfloor + J_{\mathrm{NZP},1}$ if $J^R_{\mathrm{NZP},1} = l_1 : D : N_R$ or $J_{\mathrm{NZP},n} = \beta_n - (n-1)\lfloor D/M \rfloor + J_{\mathrm{NZP},1}$ if $J^L_{\mathrm{NZP},1} = -l_1 : -D : -N_L$ where D is defined in Design 1A and β_n is chosen to satisfy $J_{\mathrm{NZPM},n} \cap J_{\mathrm{NZP},n} = \emptyset$.

Design 1E: This is a preamble-type design for estimating the main diagonal elements of $\mathbf{Q}_{ij,n}$ for K digital channels when $\rho < \mathrm{IFD}_{\mathrm{main}}$. This design applies Design 1D (requiring $M = \lceil \mathrm{IFD}_{\mathrm{main}} / \rho \rceil$ preamble symbols) for each digital channel and uses a total of MK preamble symbols. Digital channel n uses nth group of consecutive M preamble symbols.

Design 2A: This is a pilot-data multiplexed type for estimating ICI and MTI coefficients for a single digital channel. It uses $2V$ non-zero pilot tones in each pilot-data multiplexed symbol where the right side and the left side of the DC tone each has V non-zero pilot tones defined respectively by $\mathbf{p}^R = \mathbf{p}^L = [\mathbf{0}_{1\times\kappa}, \mathbf{1}_{1\times V} \otimes \mathbf{p}, \mathbf{0}_{1\times\kappa}]$ where $\otimes$ denotes the Kronecker product and $\mathbf{p}$ represents either basic pilot pattern template 1 defined by $[\mathbf{0}_{1\times\kappa}, 1, \mathbf{0}_{1\times\kappa}, \mathbf{0}_{1\times 2\iota+1}]$ or template 2 defined by $[\mathbf{0}_{1\times 2\iota+1}, \mathbf{0}_{1\times\kappa}, 1, \mathbf{0}_{1\times\kappa}]$ where 1 represents a non-zero pilot while 0 denotes a null pilot. The non-zero pilot index set due to $\mathbf{p}^R$ is given by $J^R_{\mathrm{NZP},n}$ and that due to $\mathbf{p}^L$ is given by $J^L_{\mathrm{NZP},n}$. They are related such that $-J^L_{\mathrm{NZP},n} = J^R_{\mathrm{NZP},n} + \kappa + \iota + 1$ for the basic pilot template 1 and $-J^L_{\mathrm{NZP},n} = J^R_{\mathrm{NZP},n} - \kappa - \iota - 1$ for the basic pilot template 2. In general, $\mathbf{p}^R$ and $\mathbf{p}^L$ can be positioned at any two groups of contiguous subcarriers as long as the above conditions are satisfied. Any tones from the leftmost or rightmost null pilot tones $\mathbf{0}_{1\times\kappa}$ can be skipped if they coincide with the null tones either at the band-edge or around the DC tone.

Design 2B: This is a pilot-data multiplexed type for estimating ICI and MTI coefficients for K digital channels where all non-zero and null pilots of the K channels can be inserted

within each pilot-data multiplexed symbol. Suppose digital channel i uses $2V$ non-zero pilot tones. Then, this design requires that $2(\kappa+\iota+1)VK + 2\kappa < \min(N_L, N_R)$ or $2(\kappa+\iota+1)VK + K + 2\kappa < \min(N_L, N_R)$ for a more conservative design. Define $\mathbf{p}^{R,(i)} = \mathbf{p}^{L,(i)} = [\mathbf{1}_{1\times V} \otimes \mathbf{p}]$ where $\mathbf{p}$ is defined in Design 2A. The non-zero pilot tone index sets of $\mathbf{p}^{R,(i)}$ and $\mathbf{p}^{L,(i)}$ are denoted by $J^{R,(i)}_{\mathrm{NZP},n}$ and by $J^{L,(i)}_{\mathrm{NZP},n}$, respectively. Then, this design positions $\mathbf{p}^{R,(i)}$ and $\mathbf{p}^{L,(i)}$ such that $-J^{L,(i)}_{\mathrm{NZP},n} = J^{R,(i)}_{\mathrm{NZP},n} + \kappa + \iota + 1$ for the basic template 1, and $-J^{L,(i)}_{\mathrm{NZP},n} = J^{R,(i)}_{\mathrm{NZP},n} - \kappa - \iota - 1$ for the basic template 2. $\{\mathbf{p}^{R,(i)}\}$ can be cascaded as $[\mathbf{p}^{R,(1)}, \mathbf{p}^{R,(2)}, \cdots, \mathbf{p}^{R,(K)}]$ or with 1 buffer null tone (more conservative design) as $[\mathbf{p}^{R,(1)}, 0, \mathbf{p}^{R,(2)}, 0, \cdots, \mathbf{p}^{R,(K-1)}, 0, \mathbf{p}^{R,(K)}]$. The non-zero pilot indexes of different digital channels are related by either $J^{R,(i+1)}_{\mathrm{NZP},n} = J^{R,(i)}_{\mathrm{NZP},n} + 2(\kappa+\iota+1)$ or $J^{R,(i+1)}_{\mathrm{NZP},n} = J^{R,(i)}_{\mathrm{NZP},n} + 2(\kappa+\iota+1)+1$ for the design without or with one buffer null tone, respectively. At the left side of the DC tone, $\{\mathbf{p}^{L,(i)}\}$ are cascaded in the same way except towards the left side. Next, additional contiguous null pilots are added at the right sides of $\mathbf{p}^{R,(K)}$ and $\mathbf{p}^{L,(1)}$, and at the left sides of $\mathbf{p}^{R,(1)}$ and $\mathbf{p}^{L,(K)}$.

IV. Proposed Estimators and Compensation

A. Joint Channel and RF Distortion Compensation

Based on (6), our approach first estimates significant elements of $\mathbf{Q}_n$ with the aid of two groups of pilots. The first group is in the preamble form based on Design-1. In this pilot transmission phase, based on values of κ, ι, and ρ, we choose an appropriate pilot design. The second group is in the pilot-data-multiplexed form based on Design-2. Let $\mathcal{T}_{\mathrm{pre},u_1}$ and $\mathcal{T}_{\mathrm{PDM}}$ denote the symbol index set of preamble symbols and that of pilot-data multiplexed symbols within a frame. After computing an estimate of $\mathbf{Q}_n$ for $n \in \mathcal{T}_{\mathrm{PDM}}$ (to be described in the next subsection), the compensation of the channel and RF distortion is performed by

$$\hat{\mathbf{C}}_n = \left(\hat{\mathbf{Q}}_n\right)^{\dagger} \mathbf{Y}_n \tag{7}$$

where $(.)^{\dagger}$ is the pseudoinverse operator.

B. Estimation of the Equivalent Channel Matrix

Next, we discuss estimation of $\mathbf{Q}_{u_2u_1,n}$. From (5), we need to estimate $\mathbf{U}_{u_2u_1,n}$ and $\mathbf{V}_{u_2u_1,n}$ for $\mathbf{Q}_{u_2u_1,n}$. From (2) and (3) together with the approximately-banded diagonal form of $\mathbf{A}_{u_2u_1,n}$ and the approximately anti-diagonal form of $\mathbf{B}_{u_2u_1,n}$, we see after obtaining estimate $\hat{\mathbf{U}}_{u_2u_1,n}$, we also obtain estimate $\hat{\mathbf{V}}_{u_2u_1,n}$ by multiplying the banded diagonals of $\hat{\mathbf{U}}_{u_2u_1,n}$ by j and its anti-diagonal by $-j$. We assume the channel does not change with time significantly.

Estimation of CPE-induced phase change: Based on the received pilots in both of the preamble and pilot-data multiplexed forms, we can estimate the CPE-induced phase change between an OFDM preamble symbol and a pilot-data multiplexed OFDM symbol by

$$a_{u_2u_1,n_pn_d} = \frac{\sum_{k_i \in J^{(u_1)}_{\mathrm{NZP},n_d} \cap J^{(u_1)}_{\mathrm{NZP},n_p}} \frac{Y_{u_2,n_d}[k_i] p_{n_p}[k_i]}{Y_{u_2,n_p}[k_i] p_{n_d}[k_i]}}{|J^{(u_1)}_{\mathrm{NZP},n_d} \cap J^{(u_1)}_{\mathrm{NZP},n_p}|}, \tag{8}$$

for $n_p \in \mathcal{T}_{\mathrm{pre}}$ and $n_d \in \mathcal{T}_{\mathrm{PDM}}$ where $p_n[k_i]$ represents pilot symbol transmitted on subcarrier k_i at OFDM symbol index n. Next, we can obtain the estimate of the CPE-induced phase change between two OFDM preamble symbols by

$$a_{u_2u_1,n_{p2}n_{p1}} = \mathrm{average}_{n_d}\left(\frac{a_{u_2u_1,n_{p2}n_d}}{a_{u_2u_1,n_{p1}n_d}}\right) \tag{9}$$

where $\mathrm{average}_{n_d}$ means averaging over valid values of n_d for which $|J^{(u_1)}_{\mathrm{NZP},n_d} \cap J^{(u_1)}_{\mathrm{NZP},n_p}| > 0$.

Estimation of the main diagonal elements: First, we estimate the main diagonal of $\mathbf{U}_{u_2u_1}$, or equivalently the main diagonal of $\mathbf{A}_{u_2u_1}$, at the pilot tone locations based on the preamble pilot symbols as

$$\hat{A}_{u_2u_1,n}[i,i] = \frac{Y_{u_2u_1,n}[k_i]}{p_n[k_i]}, \quad k_i \in J^{(u_1)}_{\mathrm{NZP},n}, n \in \mathcal{T}_{\mathrm{pre},u_1}. \tag{10}$$

In the case with one preamble symbol ($M = 1$), $\{\hat{A}_{u_2u_1,n}[i,i]\}$ for $k_i \notin J^{(u_1)}_{\mathrm{NZP},n}$ for $n \in \mathcal{T}_{\mathrm{pre},u_1}$ are obtained by interpolation[1] of $\{\hat{A}_{u_2u_1,n}[i,i]\}$ in (10). The main diagonal elements for symbols $n_d \in \mathcal{T}_{\mathrm{PDM}}$ are simply obtained by

$$\hat{A}_{u_2u_1,n_d}[i,i] = a_{u_2u_1,n_pn_d} \hat{A}_{u_2u_1,n_p}[i,i], \ n_p \in \mathcal{T}_{\mathrm{pre},u_1}. \tag{11}$$

In the case with $M > 1$, say $\mathcal{T}_{\mathrm{pre},u_1} = \{1, \cdots, M\}$, we use preamble symbol M as the reference and compute

$$\hat{A}_{u_2u_1,M}[i,i] = a_{u_2u_1,n_pM} \hat{A}_{u_2u_1,n_p}[i,i], \quad \forall n_p \in \mathcal{T}_{\mathrm{pre},u_1}. \tag{12}$$

This gives $\{\hat{A}_{u_2u_1,M}[i,i]\}$ for $i \in \cup_{n\in\mathcal{T}_{\mathrm{pre},u_1}} J^{(u_1)}_{\mathrm{NZP},n}$. The remaining diagonal elements at symbol M are obtained by interpolation of $\{\hat{A}_{u_2u_1,M}[i,i]\}$ obtained above. Then, the main diagonal elements are simply obtained by

$$\hat{A}_{u_2u_1,n_d}[i,i] = a_{u_2u_1,Mn_d} \hat{A}_{u_2u_1,M}[i,i], \ n_d \in \mathcal{T}_{\mathrm{PDM}}, \ \forall i. \tag{13}$$

Estimation of normalized ICI coefficients: Based on the design-2 pilots at OFDM symbol $n \in \mathcal{T}_{\mathrm{PDM}}$, we estimate the normalized ICI coefficients for those elements at an ICI spread of d tones ($d \in \{\pm 1, \cdots, \pm\kappa\}$) as

$$b^d_{u_2u_1,n} = \sum_{k_i \in J^{(u_1)}_{\mathrm{NZP},n}} \frac{Y_{u_2,n}[k_i - d]}{|J^{(u_1)}_{\mathrm{NZP},n}| \ Y_{u_2,n}[k_i]}, \quad n \in \mathcal{T}_{\mathrm{PDM}}. \tag{14}$$

Estimation of the MTI coefficient: Based on the design-2 pilots at symbol $n \in \mathcal{T}_{\mathrm{PDM}}$, we estimate MTI coefficient by

$$m_{u_2u_1,n} = \sum_{k_i \in J^{(u_1)}_{\mathrm{NZP},n}} \frac{Y_{u_2,n}[-k_i]}{|J^{(u_1)}_{\mathrm{NZP},n}| \ Y^*_{u_2,n}[k_i]}, \quad n \in \mathcal{T}_{\mathrm{PDM}}. \tag{15}$$

In (15), we only present for $\iota = 0$ since we observe $\iota = 0$ is sufficient even for large phase noise levels (see Table I).

Obtaining the banded diagonal elements (excluding main diagonal): Based on the estimates of normalized ICI

[1] We use separate interpolation for absolute values and angles based on the pchip function in MATLAB and for band-edge non-pilot sub-carriers we just use the channel estimate of the adjacent pilot tone to prevent overshoot.

coefficients, the banded diagonal elements at ICI spread of d tones ($d \in \{\pm 1, \cdots, \pm\kappa\}$) are estimated as

$$\hat{A}_{u_2u_1,n}[i-d,i] = b^d_{u_2u_1,n}\hat{A}_{u_2u_1,n}[i,i],\ n \in \mathcal{T}_{\rm PDM}. \quad (16)$$

Obtaining the anti-diagonal elements of $\hat{B}_{u_2u_1,n}$: Based on the MTI coefficient estimate, the anti-diagonal elements for $n \in \mathcal{T}_{\rm PDM}$ are estimated as

$$\hat{B}_{u_2u_1,n}[i,N-i] = m_{u_2u_1,n}\hat{A}^*_{u_2u_1,n}[N-i,N-i]. \quad (17)$$

Obtaining $\hat{\mathbf{Q}}_{u_2u_1,n}$: After obtaining estimates $\hat{\mathbf{A}}_{u_2u_1,n}$ and $\hat{\mathbf{B}}_{u_2u_1,n}$, we obtain $\hat{\mathbf{Q}}_{u_2u_1,n}$, $n \in \mathcal{T}_{\rm PDM}$, from (2), (3) and (5).

Setting κ_0, ι_0, and ρ_0: Our pilot designs are developed in a general form in terms of κ, ι, and ρ. Here we present an approach for setting their initial values. First, we obtain the probability mass function (PMF) of κ and ι by simulation for the considered system. This can be done by using a modified pilot Design 2A in a preamble format. In this modified design, V is chosen to convert to the preamble format and the non-zero pilot tone spacing at each side of the DC tone is set to be larger than $2(\kappa_{\max}+\iota_{\max}+1)$ where $\kappa_{\max}$ and $\iota_{\max}$ are the maximum values of κ and ι to be obtained for their PMF. In each realization, for a TX non-zero pilot tone n, the values of κ and ι are chosen as $\kappa = \max\{|d|\}$ such that $|Y[n \pm d]/Y[n]|^2 > \tau_{\rm th}$ (e.g., $\tau_{\rm th} = 0.003$) and $\iota = \max\{|d|\}$ such that $|Y[-n \pm d]/Y[n]|^2 > \tau_{\rm th}$. Then, the initial values κ_0 and ι_0 for the pilot designs can be set as $\min\{x\}$ such that $F(x) \geq P_{\rm th}$ (e.g., $P_{\rm th} = 0.85$) where $F(\cdot)$ is the respective cumulative distribution function of κ or ι. There exist several coherence bandwidth definitions and we use $W_{\rm coh} = 0.15/\tau_{\rm ch,rms}$ for ρ_0, where $\tau_{\rm ch,rms}$ is the root mean-square channel delay spread.

V. Numerical Results and Discussion

We compare the BER performance between the proposed design and two existing approaches in [10] (reference design 1) and [3] (reference 2). We consider a downlink OFDM with 64 TX antennas and 4 receive antennas at a carrier frequency of 73 GHz. The channel model is based on the 3GPP LTE channel model with two clusters where each cluster has 20 sub-paths, the second clusters delay is about 80 ns and its power is -9 dB with reference to the first cluster. Analog beamforming applies a phase shift beamformer (delay-and-sum beamforming [12]) in the direction of the average arrival angle of the 20 sub-paths of the first cluster where we assume such average arrival angle is known (can be estimated in an earlier phase). We simply consider a single digital channel with 16-QAM under two system settings; System-1 uses $N_{\rm DFT} = 256$, $\Delta f = 1.44$ MHz, and the signal bandwidth of 250 MHz[2] (168 used subcarriers excluding the DC tone). System-2 has $N_{\rm DFT} = 512$, $\Delta f = 720$ kHz, and the signal bandwidth of 250 MHz (336 used subcarriers excluding the DC tone).

The signals are generated in time domain with 4 times oversampling as in Fig. 1, while our pilot designs, estimation and compensation are based on frequency domain model in Section II. The PN power spectral densities at TX and RX sides are independently modeled as $\mathrm{PSD}(f) = \mathrm{PSD}(0)[1 + (\frac{f}{f_z})^2]/[1 + (\frac{f}{f_p})^2]$ where PSD(0) = -60 dBc/Hz, PSD(100k) = -70 dBc/Hz and PSD(∞) = -130 dBc/Hz. The CFOs at TX and RX sides are independently and uniformly distributed within the range of ± 1 ppm, the receiver SFO is set at 1ppm and the receiver STO is uniformly distributed within $[-T_{\rm rx}/2, T_{\rm rx}/2]$ where $T_{\rm rx}$ is the receive sampling period. IQIs are independent at the TX and RX sides and they are uniformly distributed within the range defined by the maximum amplitude imbalance of 4 dB and the maximum phase imbalance of 5 degrees. The nonlinear power amplifier model is according to IEEE 802.11ad with 9 dB output power backoff. The mobile speed is 10 km/h. The average SNR (per tone defined over used data tones) is set at 10 dB. The transmission frame has 7 OFDM symbols for reference 1 and the proposed method, and 5 symbols for reference 2 in order to keep similar pilot overhead. The proposed design uses $M = 1$ preamble symbol (Design 1A) followed by pilot-data multiplexed symbols where pilots are based on Design 2A with $V = 3$ (i.e., 6 non-zero pilot tones in each pilot-data multiplexed symbol). The reference 1 assumes small PN and IQI at the RX side, and uses one preamble, and some scattered pilots in the later OFDM symbols, and its pilot overhead is kept the same as the proposed method with $M = 1$ case. The reference 2 applies two preamble symbols at the beginning of the frame and its pilot overhead is higher than the proposed method with $M = 1$ case.

We first discuss the initial setting of κ and ι. We use a preamble with non-zero pilots at tone indexes $[-74, -32, 11, 53]$. The PMFs obtained from 20,000 realizations are shown in Table I, based on which we set $\kappa_0 = 3$ and $\iota_0 = 0$ for $\Delta f = 720$ kHz and $\kappa_0 = 2$ and $\iota_0 = 0$ for $\Delta f = 1.44$ MHz. Per our design guideline, a few values of κ and ι around their initial values should be tested.

Fig. 4 presents the uncoded BER performance of the proposed design with different settings of κ (with $\iota = 0$) and M (# preamble symbols due to different settings of ρ) for the system with $\Delta f = 720$ kHz. With $M = 1$ preamble symbol, increasing κ from 2 to 4 improves BER as ICI effect on channel estimation is lessened but when $\kappa = 5$, BER degrades. The reason is that $\kappa = 5$ results in the boundary condition $\rho = \mathrm{IFD}_{\rm main}$ between design 1A ($M = 1$) and design 1D ($M > 1$), and the channel interpolation performance appears to get affected due to a larger pilot tone spacing. In the case with $\kappa = 5$, design 1D with $M = 2$ should also be tested, and its uncoded BER results in Fig. 4 show that $M = 2$ is better for $\kappa = 5$. Overall, the BER results show that $\kappa = 4$ is the best choice for the system with $\Delta f = 720$ kHz.

Next, in Fig. 5 for the system with $\Delta f = 720$ kHz, we present uncoded BER comparison between the proposed pilot design ($\kappa = 4$, $\iota = 0$, $M = 1$) and two reference designs. We can see that the reference designs fail to perform well, while the proposed design has much better performance.

For the system with $\Delta f = 1.44$ MHz, we present uncoded

[2]We also investigated with 2 GHz bandwidth using the same sub-carrier spacings and the performance comparison results are similar for the initial tested cases. But due to their much longer simulation time and various settings to test, we used a bandwidth down-scaled system with 250 MHz bandwidth.

TABLE I
PMF OF κ AND ι

Δf	κ or ι	0	1	2	3	4	5	6	7	8	9	10
720 kHz	PMF(κ)	0.1001	0.4949	0.2263	0.1093	0.0459	0.0143	0.0051	0.0016	0.0011	0.0004	0.0011
720 kHz	PMF(ι)	0.8576	0.1384	0.0014	0.0001	0.0001	0.0001	0.0001	0.0001	0.0003	0.0004	0.0015
1.44 MHz	PMF(κ)	0.1043	0.6040	0.2700	0.0172	0.0021	0.0006	0.0002	0.0002	0.0002	0.0004	0.0007
1.44 MHz	PMF(ι)	0.8597	0.1380	0.0003	0.0001	0.0000	0.0001	0.0002	0.0001	0.0002	0.0004	0.0009

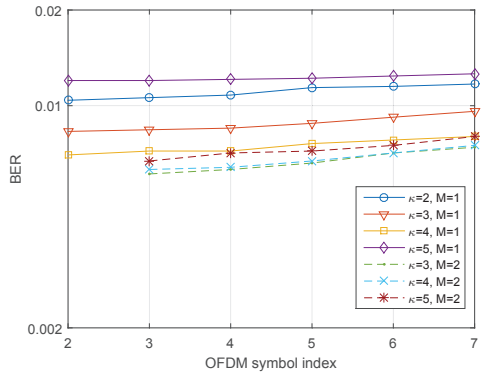

Fig. 4. Effect of κ and M on uncoded BER performance of the proposed design ($\Delta f = 720$ kHz)

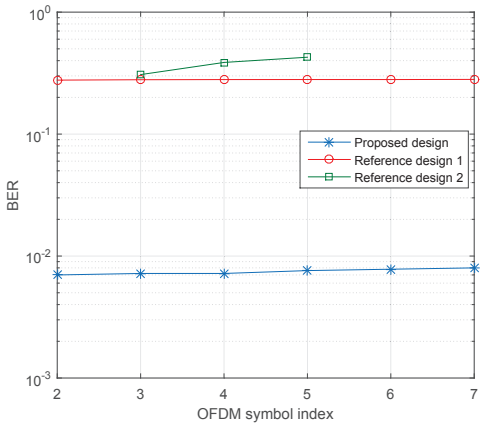

Fig. 5. Uncoded BER performance of proposed pilot design and compensation scheme for the system with $\Delta f = 720$ kHz ($\kappa = 4$, $\iota = 0$, $M = 1$)

BER comparison between the proposed pilot design ($\kappa = 2$, $\iota = 0$, $M = 1$ or $M = 2$) and two reference designs. The proposed design significantly outperforms the reference schemes. Also we note that using $M = 2$ for the proposed design notably enhances BER over the $M = 1$ case, and hence $\kappa = 2$ and $M = 2$ could be chosen for the system with $\Delta f = 1.44$ MHz if the frame length is not too short. In all results, slight increase of BER across time is due to the lack of channel tracking for time-varying channels.

VI. CONCLUSIONS

We proposed novel pilot designs and estimators for joint channel and RF distortion compensation in millimeter-wave massive MIMO systems under strong RF distortions at both the TX and RX sides. Existing pilot designs were not developed for systems with strong RF distortions. Thus, their BER performances are severely affected by strong RF distortions.

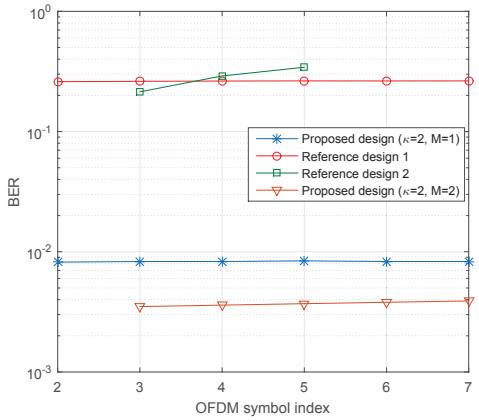

Fig. 6. Uncoded BER performance of proposed pilot design and compensation scheme for the system with $\Delta f = 1.44$ MHz

By incorporating characteristics of the strong RF distortions, the proposed designs enable reliable millimeter-wave systems under high RF distortions which can also be translated into lower transceiver RF front-end cost.

Acknowledgment: This work is partially supported by Huawei Technologies Co., Ltd., China.

REFERENCES

[1] S. Rangan, et al., "Millimeter-wave cellular wireless networks: Potentials and challenges," *Proc. IEEE*, vol. 102, no. 3, pp. 366–385, Mar. 2014.
[2] A. Tarighat, et al., "Compensation schemes and performance analysis of IQ imbalances in OFDM receivers," *IEEE Trans. Signal Process.*, vol. 53, no. 8, pp. 3257–3268, Aug. 2005.
[3] Y. Li, et al., "A new method to simultaneously estimate TX/RX IQ imbalance and channel for OFDM systems," in *IEEE ICC*, June 2013, pp. 4551–4555.
[4] W. Kirkland and K. Teo, "I/Q distortion correction for OFDM direct conversion receiver," *Electron. Lett*, vol. 39, no. 1, pp. 131–133, 2003.
[5] H. Minn and D. Munoz, "Pilot designs for channel estimation of MIMO OFDM systems with frequency-dependent I/Q imbalances," *IEEE Trans. Commun.*, vol. 58, no. 8, pp. 2252–2264, Aug. 2010.
[6] L. Brötje, et al., "Estimation and correction of transmitter-caused I/Q imbalance in OFDM systems," in *Intl. OFDM workshop*, Sept. 2002, pp. 178–182.
[7] Y. Egashira, et al., "A novel IQ imbalance compensation method with pilot-signals for OFDM system," in *IEEE VTC*, Sept. 2006.
[8] N. Kolomvakis, et al., "IQ imbalance in multiuser systems: Channel estimation and compensation," *IEEE Trans. Commun.*, vol. 64, no. 7, pp. 3039–3051, July 2016.
[9] H. Huang, et al., "Phase noise and frequency offset compensation in high frequency MIMO-OFDM system," in *IEEE ICC*, 2015, pp. 1280–1285.
[10] P. Rabiei, et al., "Reduced-complexity joint baseband compensation of phase noise and I/Q imbalance for MIMO-OFDM systems," *IEEE Trans. Wireless Commun.*, vol. 9, no. 11, pp. 3450–3460, Nov. 2010.
[11] Q. Zou, et al., "Joint compensation of IQ imbalance and phase noise in OFDM wireless systems," *IEEE Trans. Commun.*, vol. 57, no. 2, pp. 404–414, Feb. 2009.
[12] H. Van Trees, "Optimum Array Processing", New York: Wiley-Interscience, 2002.